AD-A063 142 AIR FORCE GEOPHYSICS LAB HANSCOM AFB MASS F/G 3/2
FLARES, FORCE-FREE FIELDS, EMERGING FLUX, AND OTHER PHENOMENA I--ETC(U)
AUG 78 D F NEIDIG, H L DEMASTUS, P H WIBORG

UNCLASSIFIED AFGL-TR-78-0194 NL

| OF |
AD
A063142

END
DATE
FILMED
3-79
DDC

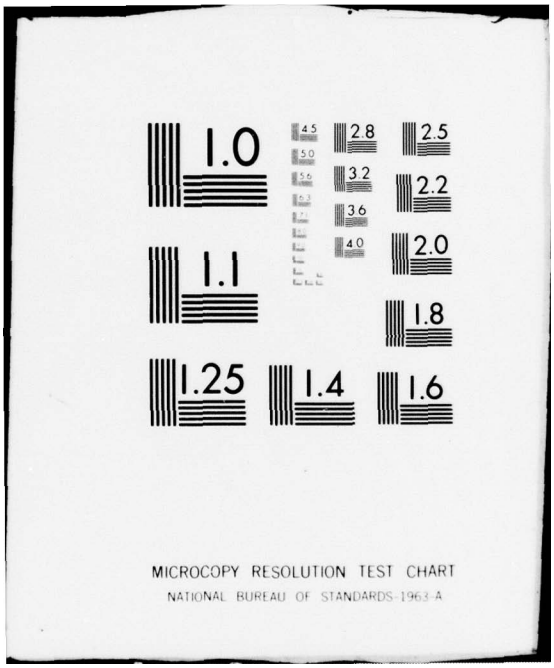
1.0
1.1
1.25
1.4
1.6
1.8
2.0
2.2
2.5
2.8
3.2
3.6
4.0
4.5
5.0
5.6
6.3
MICROCOPY RESOLUTION TEST CHART
NATIONAL BUREAU OF STANDARDS-1963-A

AFGL-TR-78-0194
ENVIRONMENTAL RESEARCH PAPERS, NO. 637






# Flares, Force-Free Fields, Emerging Flux, and Other Phenomena in McMath 14943 (September 1977)

DONALD F. NEIDIG
HOWARD L. DE MASTUS
PHILIP H. WIBORG

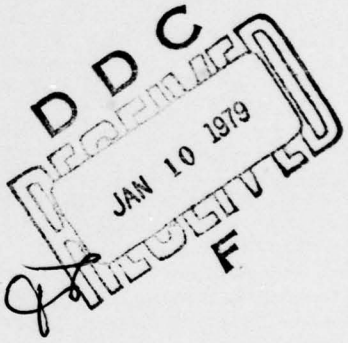


9 August 1978





SPACE PHYSICS DIVISION PROJECT 2311
AIR FORCE GEOPHYSICS LABORATORY
HANSCOM AFB, MASSACHUSETTS 01731

AIR FORCE SYSTEMS COMMAND, USAF

This report has been reviewed by the ESD Information Office (OI) and is releasable to the National Technical Information Service (NTIS).

This technical report has been reviewed and
is approved for publication.

FOR THE COMMANDER

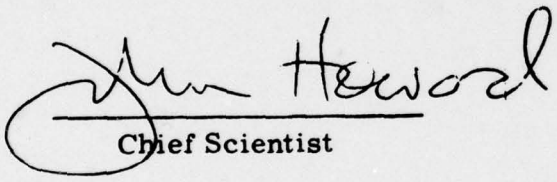

Chief Scientist

Qualified requestors may obtain additional copies from the Defense Documentation Center. All others should apply to the National Technical Information Service.

SECURITY CLASSIFICATION OF THIS PAGE (When Data Entered)

## REPORT DOCUMENTATION PAGE

READ INSTRUCTIONS BEFORE COMPLETING FORM

(14) 1. REPORT NUMBER: AFGL-TR-78-0194 > AFGL-ERP-637

2. GOVT ACCESSION NO.

3. RECIPIENT'S CATALOG NUMBER

(6) 4. TITLE (and Subtitle): FLARES, FORCE-FREE FIELDS, EMERGING FLUX, AND OTHER PHENOMENA IN McMATH 14943 (SEPTEMBER 1977)

5. TYPE OF REPORT & PERIOD COVERED: Scientific. Interim.

6. PERFORMING ORG. REPORT NUMBER: ERP No. 637

(10) 7. AUTHOR(s): Donald F. Neidig, Howard L. DeMastus, Philip H. Wiborg

8. CONTRACT OR GRANT NUMBER(s)

9. PERFORMING ORGANIZATION NAME AND ADDRESS: Air Force Geophysics Laboratory (PHS), Hanscom AFB, Massachusetts 01731

10. PROGRAM ELEMENT, PROJECT, TASK AREA & WORK UNIT NUMBERS: (16) 61102F 2311G309 (17) G3

11. CONTROLLING OFFICE NAME AND ADDRESS: Air Force Geophysics Laboratory (PHS), Hanscom AFB, Massachusetts 01731

(11) 12. REPORT DATE: 9 August 1978

13. NUMBER OF PAGES: 34

14. MONITORING AGENCY NAME & ADDRESS (if different from Controlling Office)

15. SECURITY CLASS. (of this report): Unclassified

15a. DECLASSIFICATION/DOWNGRADING SCHEDULE

16. DISTRIBUTION STATEMENT (of this Report)

Approved for public release; distribution unlimited.

17. DISTRIBUTION STATEMENT (of the abstract entered in Block 20, if different from Report)

(9) Environmental research papers

18. SUPPLEMENTARY NOTES

(12) 35 p.

19. KEY WORDS (Continue on reverse side if necessary and identify by block number)

Solar activity
Flare forecasting

20. ABSTRACT (Continue on reverse side if necessary and identify by block number)

Magnetic and photographic data covering the transit of McMath 14943 are analyzed and compared with the evolution of flare activity in the region. Several zones of concentrated flare activity are identified and found to be associated with the presence of emerging flux, sunspot motions, and sheared magnetic fields. For two flares we identify the preflare energy build-up in force-free fields as well as the relaxation of the same fields following the energy release.

DD FORM 1 JAN 73 1473 EDITION OF 1 NOV 65 IS OBSOLETE

Unclassified

SECURITY CLASSIFICATION OF THIS PAGE (When Data Entered)



409 578

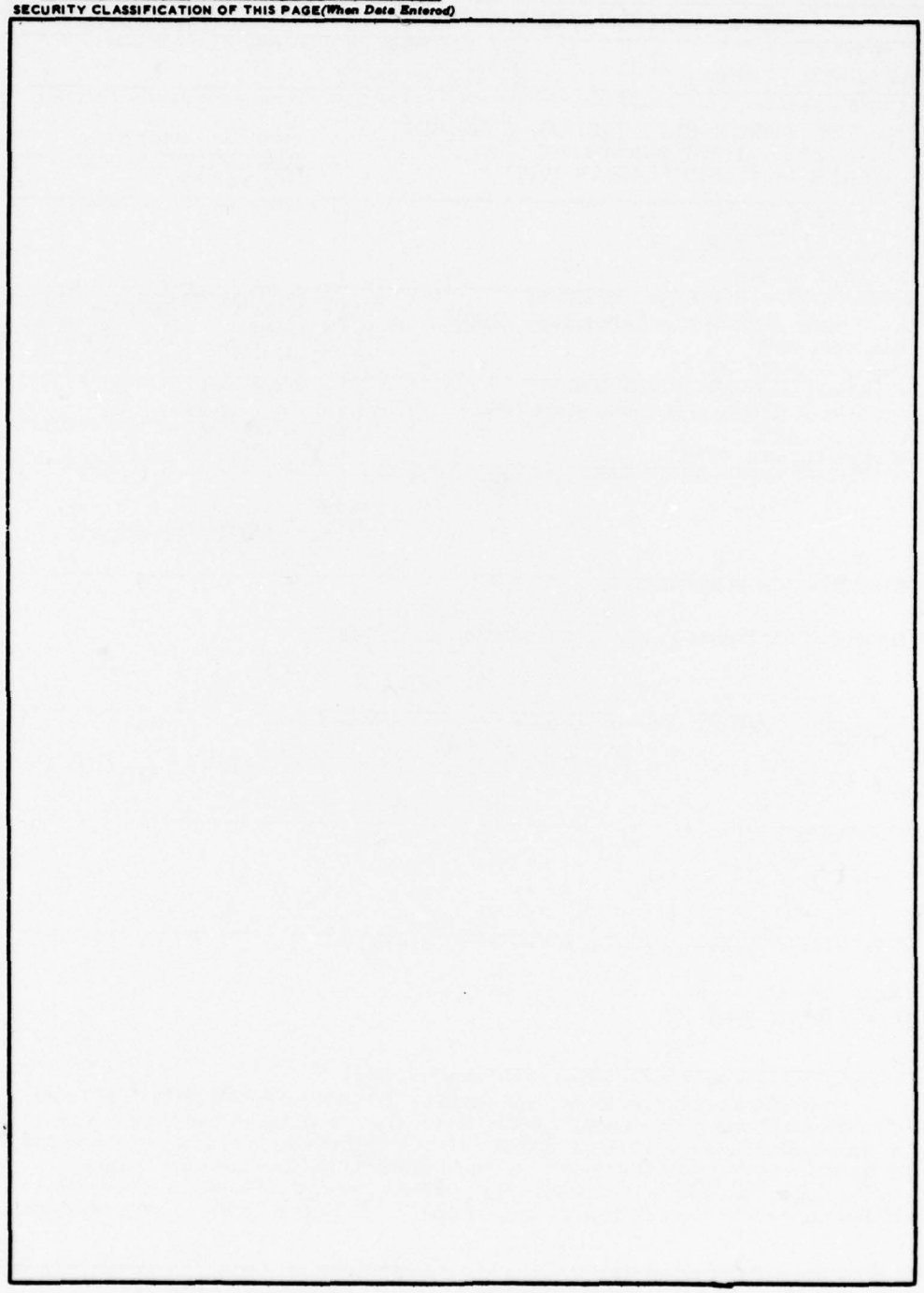

## Contents

## Illustrations



## Tables

# Flares, Force-Free Fields, Emerging Flux, and Other Phenomena in McMath 14943 (September 1977)

## 1. INTRODUCTION

We present a study of the general trend of flare activity in McMath 14943 in relation to the magnetic and dynamical evolution of the active region. It is of particular interest to discover the conditions necessary to produce flare activity. At the same time it is also important to know whether some of these same conditions are present at times and places where flares are not occurring, an obvious prerequisite in any viable scheme for flare forecasting. Of course, we are not able to comprehensively study all aspects of the active region evolution, but we do examine in particular the following phenomena which have previously been associated with flares:

(1) Sunspot motions and rotations, [1,2,3,4,5]

(2) Sheared magnetic fields, as produced by sunspot motions and rotations, [6,7,8]

(3) Evolution of principal spots, especially increases in spot areas, [9]

(4) Evolution of small-scale structures, notably the emergence of pores, [13]

(5) Emerging flux and evolving magnetic features. [11,12,13,14]

The magnetograms used in this study were obtained with the non-saturating Doppler-Zeeman Analyzer at Sacramento Peak Observatory. [15] The study of the magnetic evolution of the active region was hampered by poor time resolution

(Received for publication 9 August 1978)

(Because of the large number of references cited above, they will not be listed here. See References, page 33, for References 1 through 15.)

(several magnetograms per day). Thus, changes in field strengths and gradients occurring on time scales on the order of 1 hr could not be detected.

Photographic data were obtained from the Sacramento Peak Hα patrol (both line center and Hα ± 1 Å) and white light patrol, covering the entire transit of McMath 14943. During 13 and 14 September observations were also made with the Vacuum Tower Telescope using the Universal Birefringent Filter[16] at wavelengths of Hα and continuum near Hα. In addition to these observations the occurrences and locations of flares were obtained from Solar Geophysical Data.[17]

## 2. GENERAL DESCRIPTION OF McMATH 14943

McMath 14943 (transit dates: 8 to 22 September 1977) was magnetically complex, with polarities reversed in comparison to active regions in the solar northern hemisphere for cycle 21. With the preceding spot of negative polarity and positioned at a low solar latitude (~8 N), the region was thus characteristic of a remnant cycle 20. The spot group was classified EKC (McIntosh three-parameter classification) on nine days of its transit, indicative of a relatively high degree of flare productivity.[18] The principal magnetic inversion line was oriented east-west, also characteristic of flare-producing active regions.[5]

Several important evolutions occurred within the region during its transit. A shear-producing rotation, centered approximately on the large preceding spot, was associated with the onset of flare activity after 15 September. The reader may refer to the white light patrol photographs (Figure 1) and observe in a glance that spot B rotates around spot A in a counterclockwise sense. Also evident in the photographs is the growth and decay of several of the spots (A, B, C, D, and F) in the rotating part of the region; this growth and decay occurs nearly simultaneously with the rotation. The spots in the eastern (trailing) part of the region do not participate in the rotation but fall behind the rotating group as the latter moves forward in Carrington longitude. The appearance of the region in Hα for several days near central meridian transit, including a filtergram showing one of the large flares, is shown in Figures 2 and 3. The evolution of the magnetic configuration is derived from a series of magnetograms in Figure 4. In the following sections we consider these and other evolutions in more detail, particularly noting how each is related to both the presence and absence of flare activity.

---

16. Beckers, J.M., Dickson, L., and Joyce, R.S. (1975) AFCRL-TR-75-0090.
17. Solar Geophysical Data, World Data Center A, National Oceanic and Atmospheric Administration, Boulder, CO.
18. McIntosh, P.S. (1977) Bull. Am. Astron. Soc. 9:330.

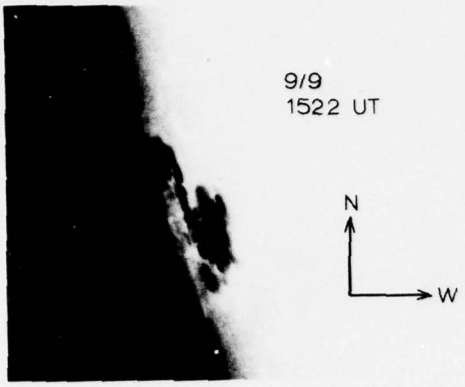


Figure 1a.

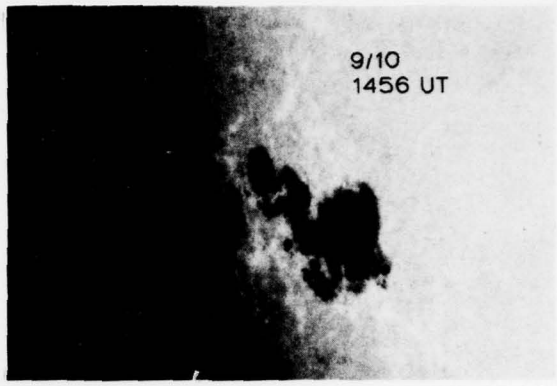


Figure 1b.

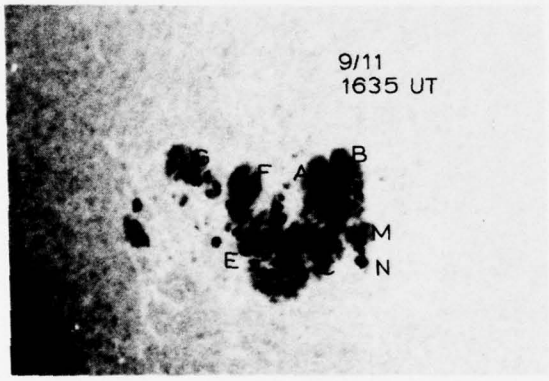


Figure 1c.

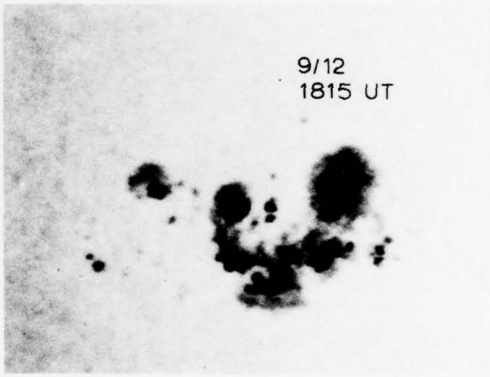


Figure 1d.

Figure 1. White Light Patrol Photographs Covering the Transit of McMath 14943 (see Figure 3 for 13 and 14 September). Spots of positive magnetic polarity are: C, D, E, J, K, M, and N. Spots of negative polarity are: A, B, F, G, H, and L

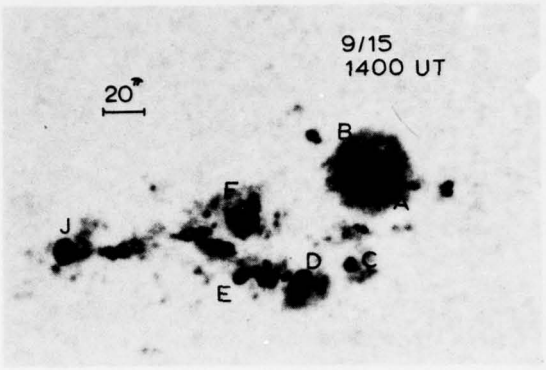


Figure 1e.

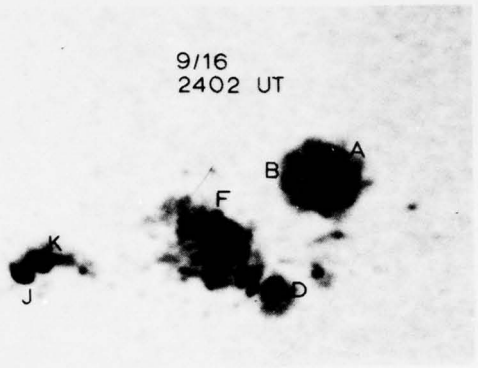


Figure 1f.

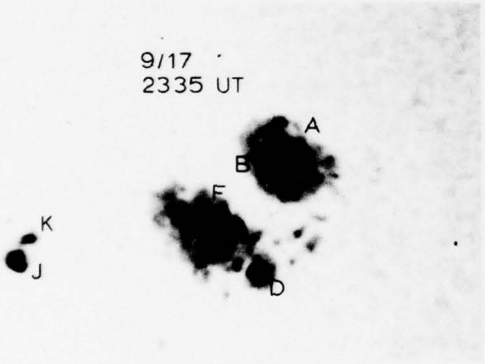


Figure 1g.

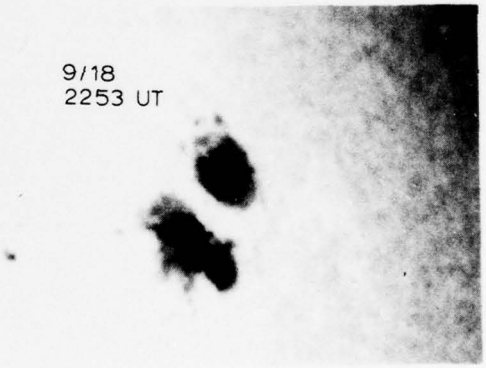


Figure 1h.

Figure 1. (Cont)

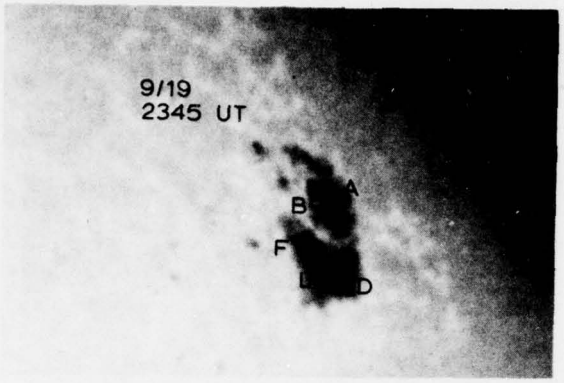


Figure 1i.


Figure 1j.

Figure 1. (Cont)

Figure 2a.

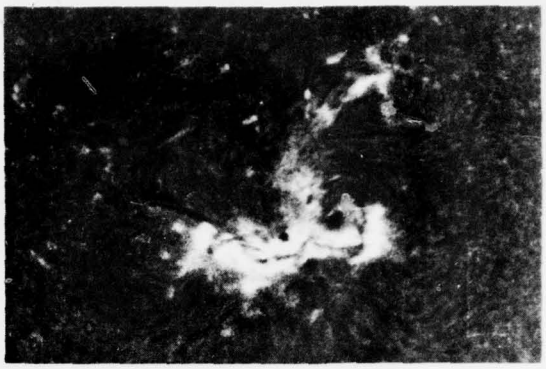

Figure 2b.

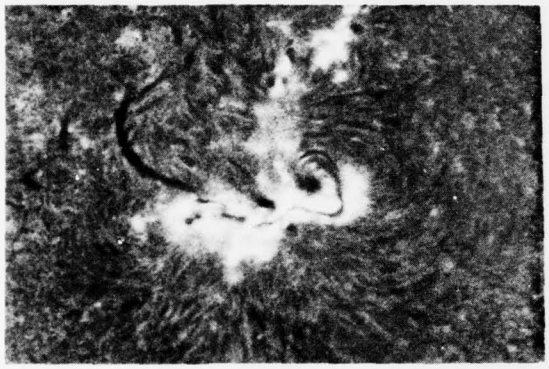

Figure 2c.

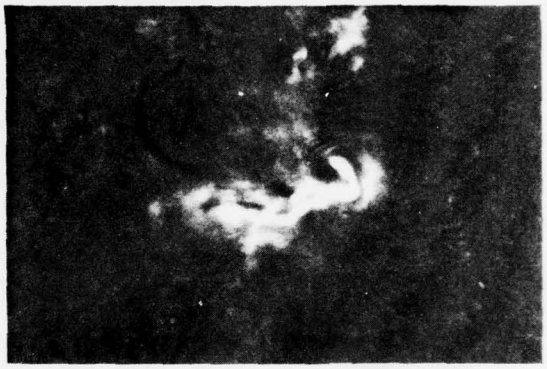

Figure 2d.

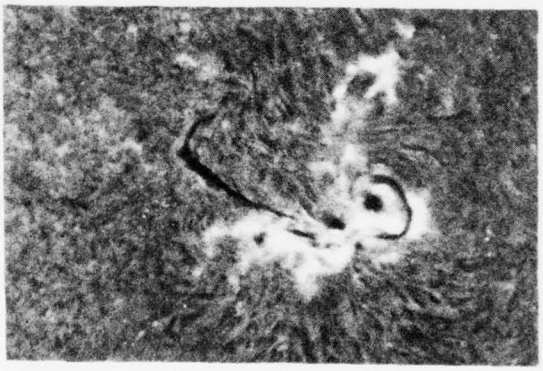

Figure 2e.

Figure 2. Hα Patrol Filtergrams Showing the Flare of 16 September and the Changes in the Neutral Line Filament Before and After the Flare. Note the westward displacement of the upper flare ribbon, indictative of the shear existing along the neutral line. Dates and times are respectively, 14 September 2311 UT, 15 September 1945 UT, 16 September 2025 UT, 16 September 2145 UT, 17 September 1335 UT. North is at the top, west to the right

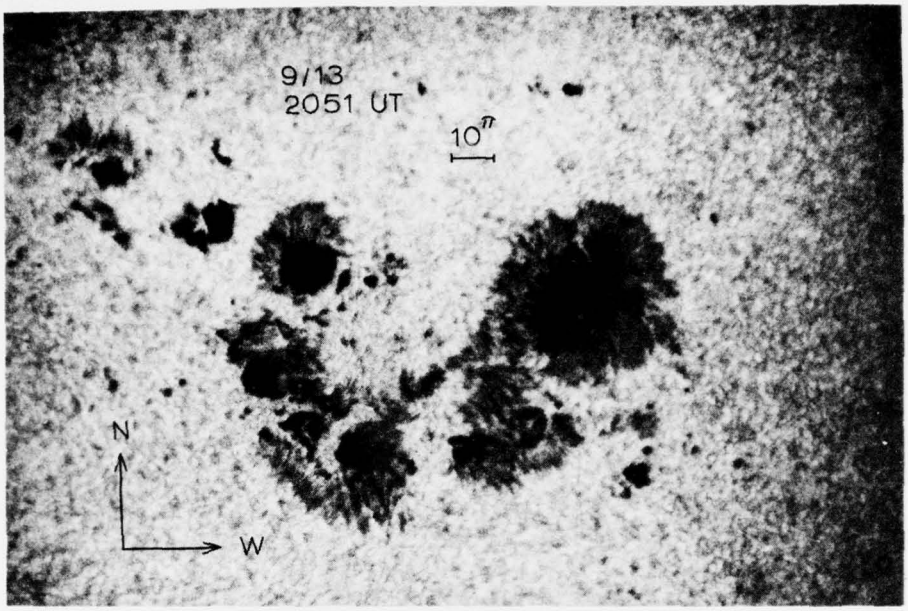


Figure 3a.

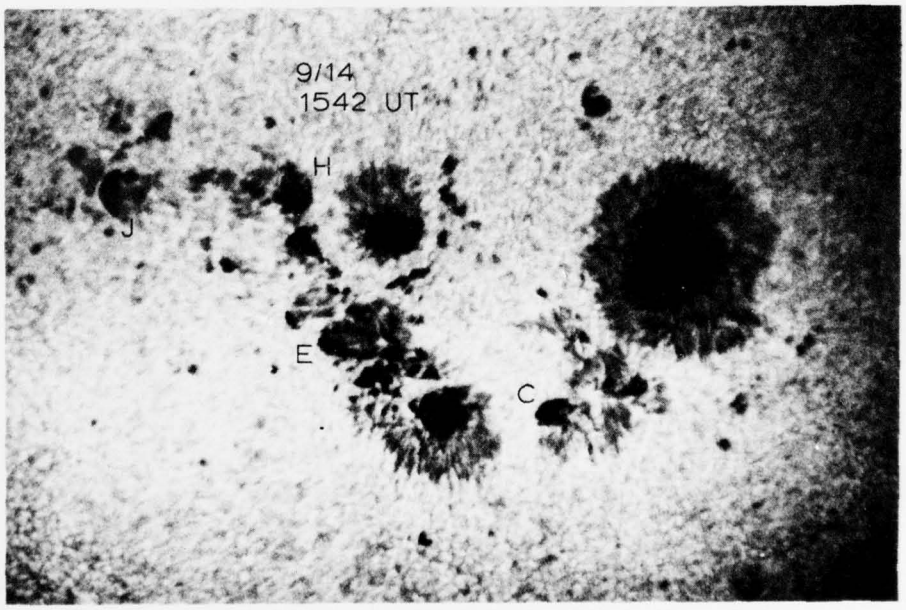


Figure 3b.

Figure 3. High Resolution Filtergrams in Hα and Continuum Near Hα

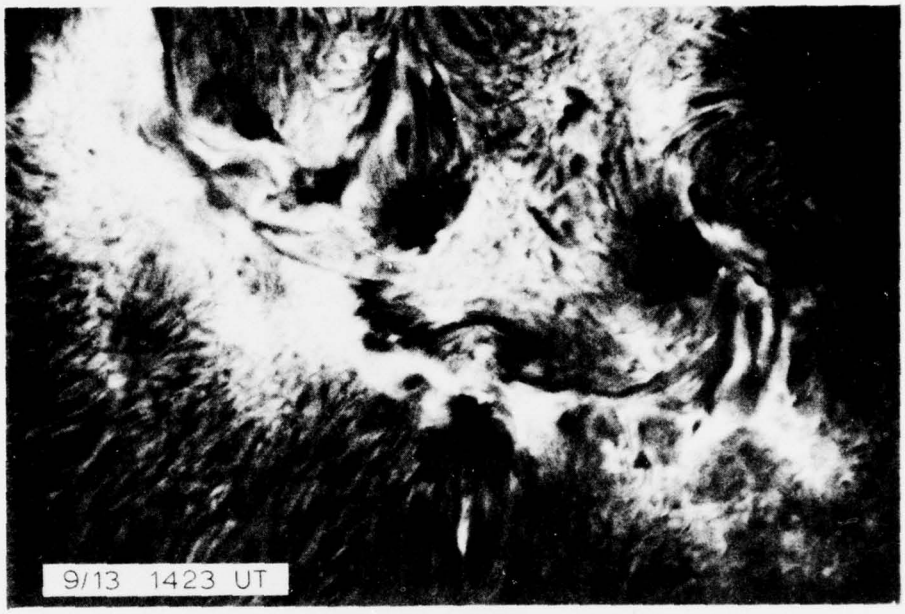


Figure 3c.

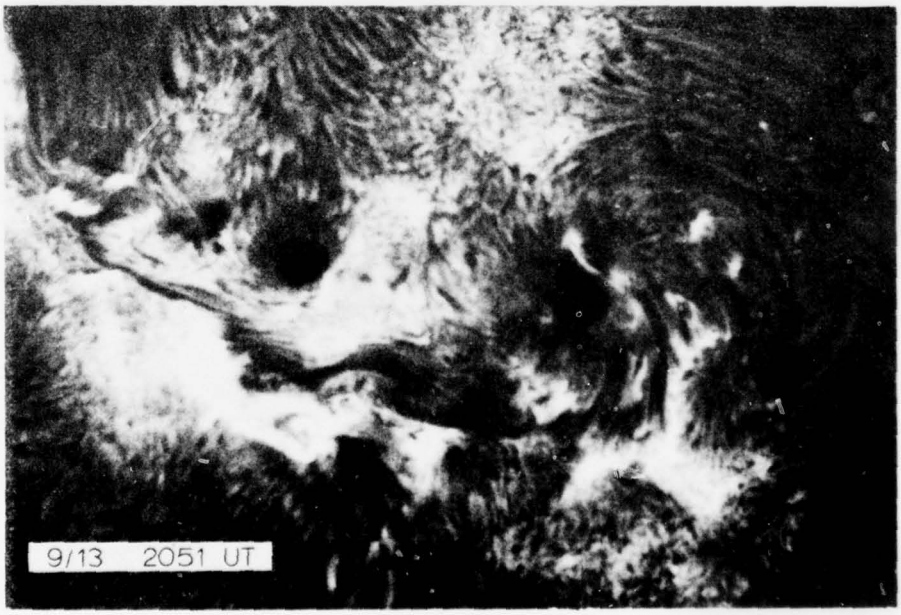


Figure 3d.

Figure 3. (Cont)

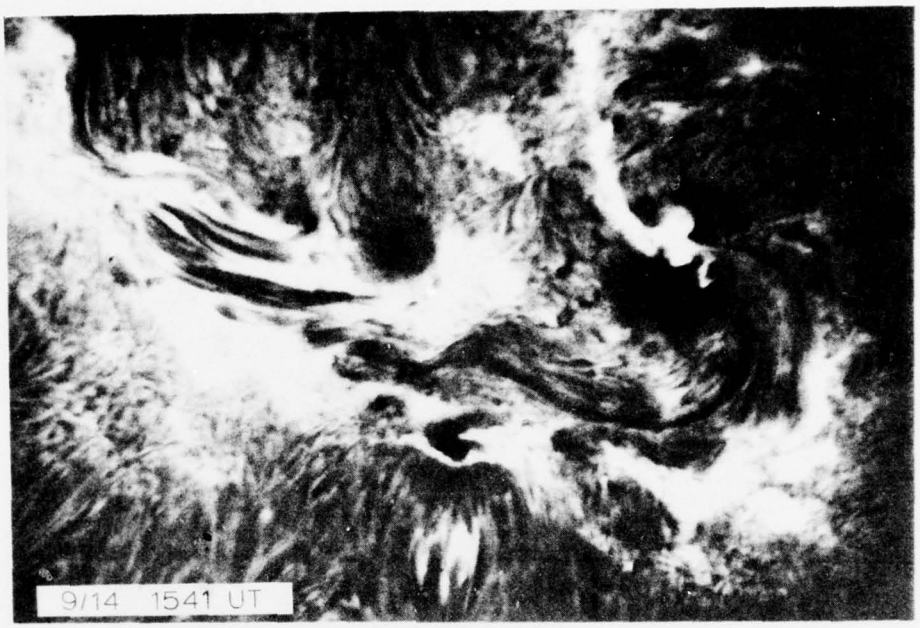


Figure 3e.

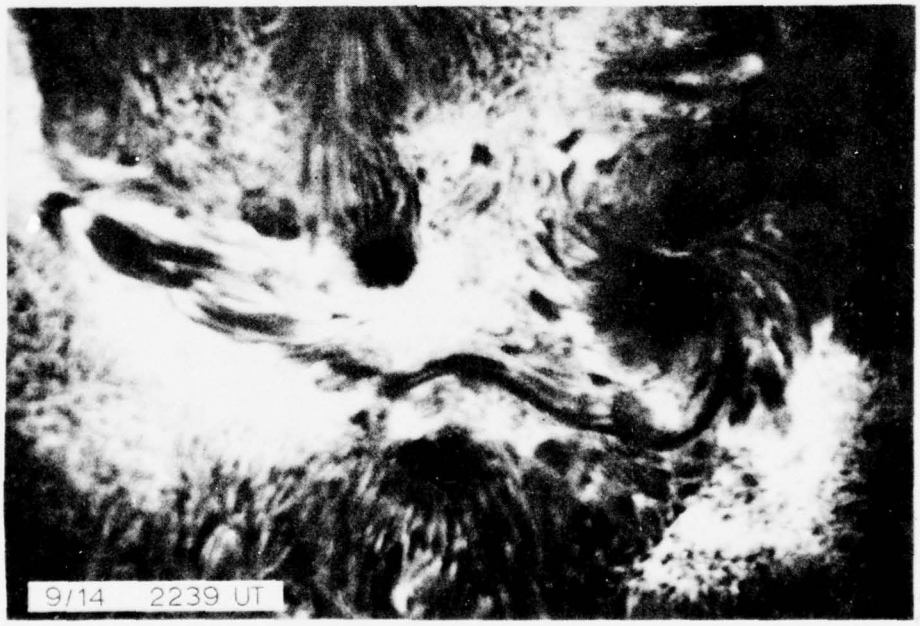


Figure 3f.

Figure 3. (Cont)

9/13 1751 UT

Figure 4a.

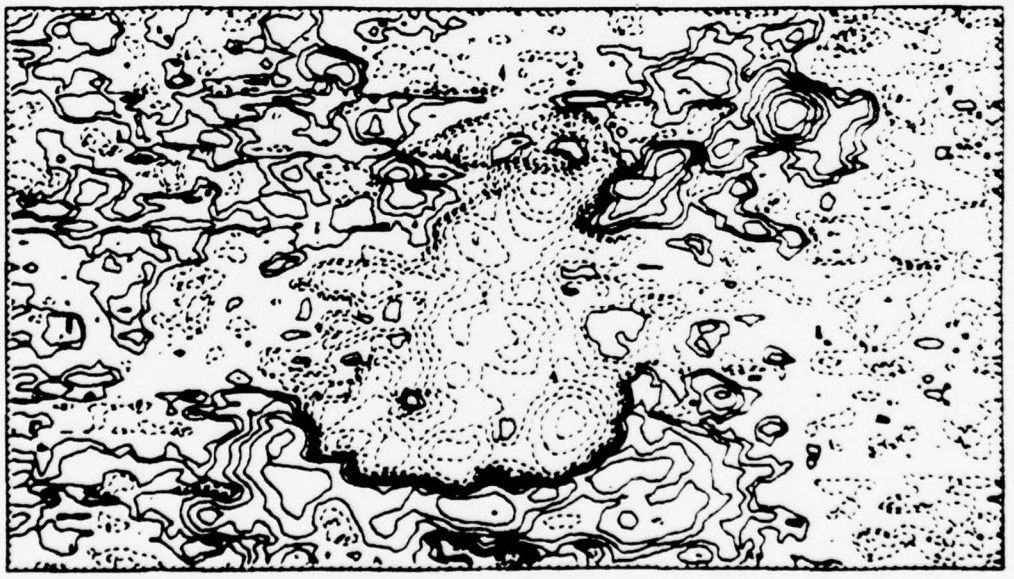

9/13 2021 UT

Figure 4b.

Figure 4. Magnetograms With Isogauss Contours $10 \times 2^{n-1}$ Gauss (n > 1, 2, 3, ...). Solid contours indicate positive polarity. Tic marks are in steps of the scanning aperture, about 5 arcsec square. North is at the top, west to the right

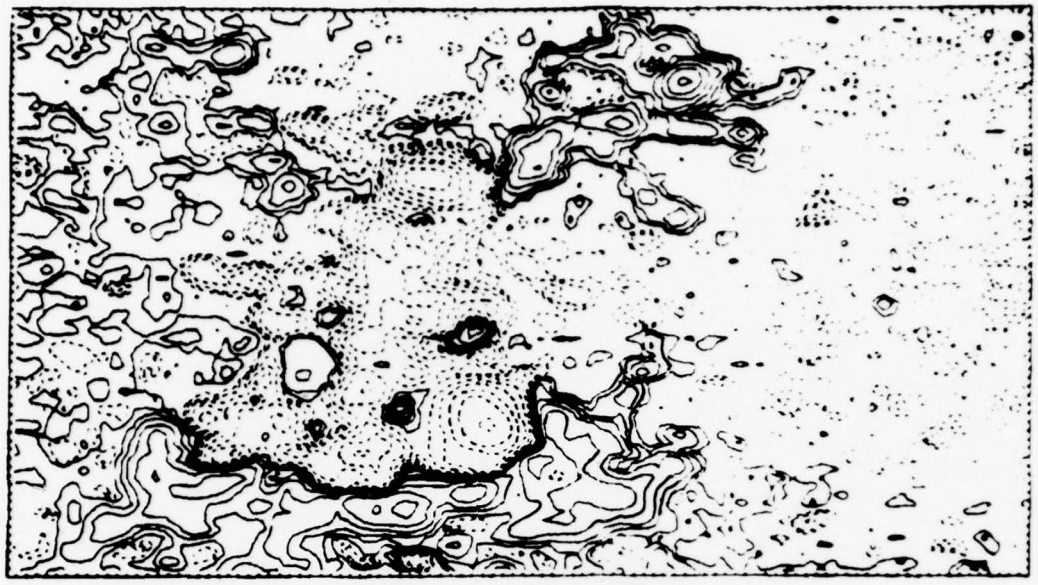


Figure 4c.

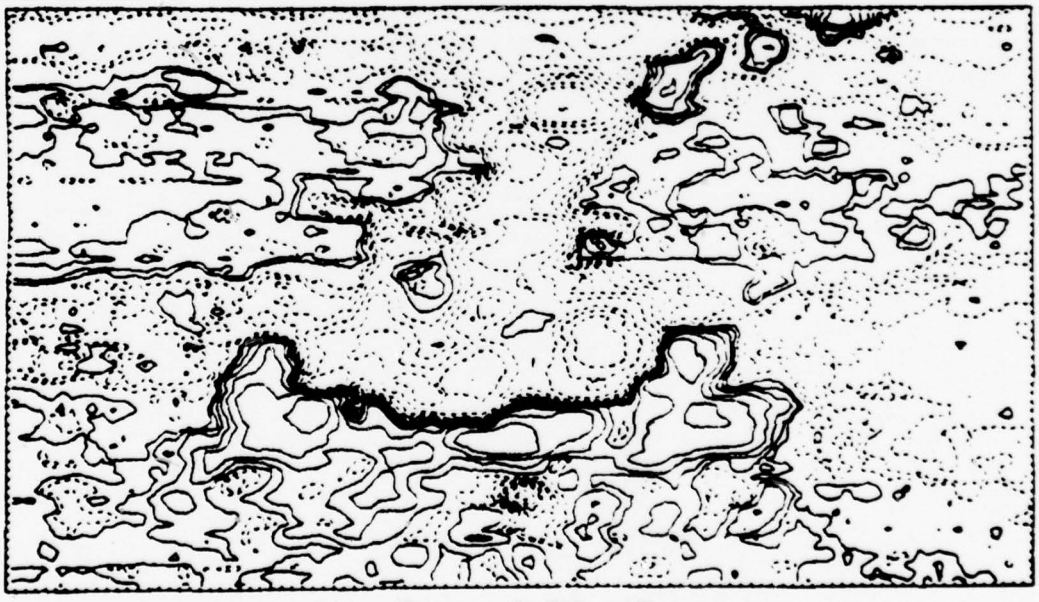


Figure 4d.

Figure 4. (Cont)

9/16 2040 UT

Figure 4e.

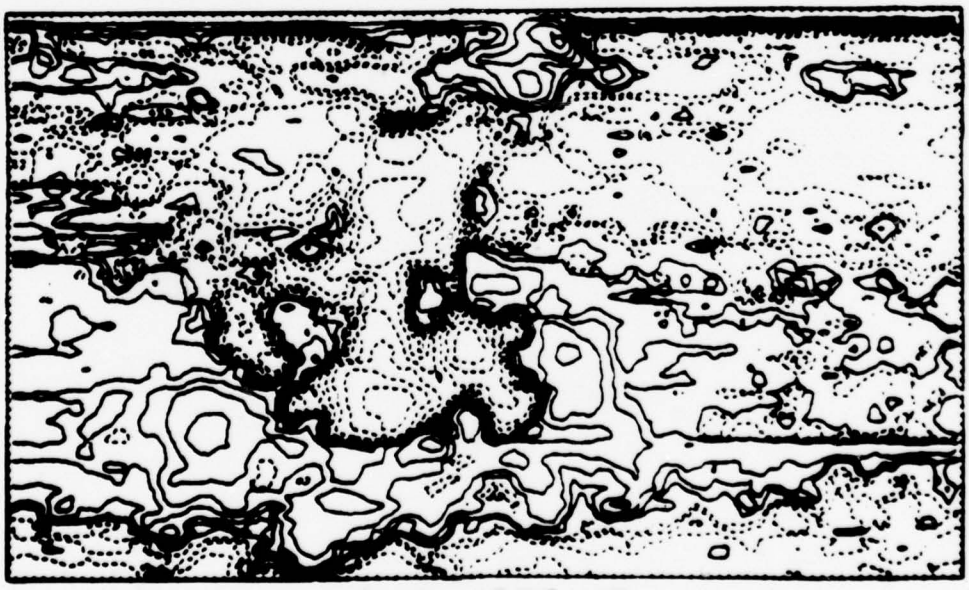

9/17 1859 UT

Figure 4f.

Figure 4. (Cont)


Figure 4g.

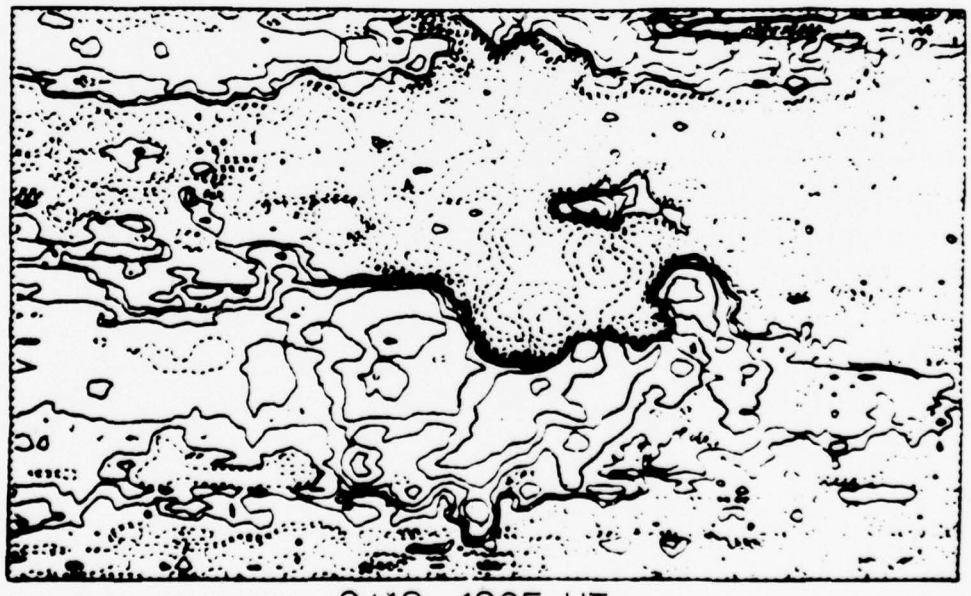


Figure 4h.

Figure 4. (Cont)

## 3. FLARE ACTIVITY

The evolution of flare activity in both time and location is depicted in Figures 5 and 6. The most obvious evolution is the shift in the relative longitude of flare centroids after 15 September. This shift appears to result from a cessation of flares in the eastern part of the region combined with an increase in flare activity in the west. The sudden decrease of flare activity in the east on 15 September, where previously there existed a locality of flare centroids tightly clustered around latitude 9N at 9 deg east of spot A, leads us to identify this location as a specific zone of concentrated flare activity, hereafter called Zone 1. From 16 to 19 September the flares are suddenly concentrated near the neutral line south of spot A which we will call Zone 2. An additional, and very abrupt, shift in the flare locations occurs during 20 and 21 September, when the flare centroids are found to be concentrated north of spot A (Zone 3). The locations of the centers of these zones are shown in Figure 7b.

The break in activity on 12 September occurs at a time when the average flaring rate is five per day; thus the absence of flares for one day can be accounted for by a $2\sigma$ fluctuation, and therefore the break in activity may not be significant. Likewise, there may be no significance in the apparent drift in longitude of flare centroids during 9 to 11 September.

Three importance 1 flares occurred in the eastern parts of the region early in the transit (9 and 10 September). Thereafter, nothing larger than subflares occurred anywhere in the region until after meridian passage when several large flares (2N, 1N, 3B) occurred in the west (16, 18, and 19 September respectively). One 2N flare occurred on 20 September in the eastern part of the region, which by this time was almost devoid of all flare activity.

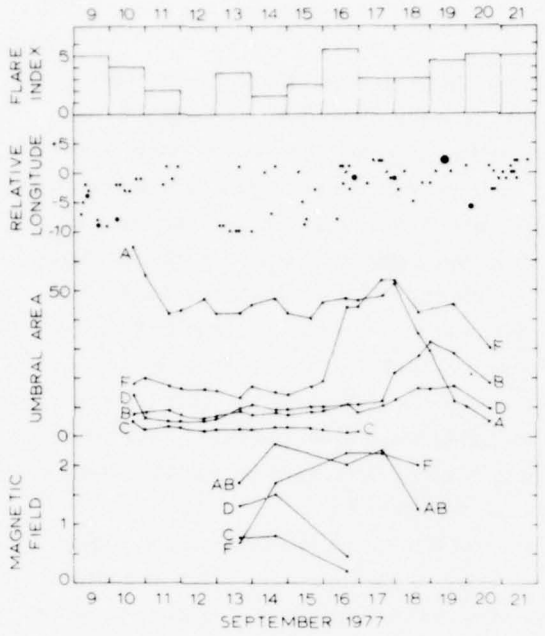


Figure 5. Trends of Activity in McMath 14943. (a) The daily flare index is the sum of the importances of all flares occurring on the particular day (subflares were assigned an importance of 1/2). (b) Longitudes of flare centroids relative to the large preceding spot. Dot sizes increase with flare importance. (c) Umbral areas (in millionths of the solar hemisphere) of the major spots, corrected for foreshortening. (d) Magnetic field strength (kG) in the major spots, measured with 5 arcsec aperture. Flare data in (a) and (b) are according to Solar Geophysical Data

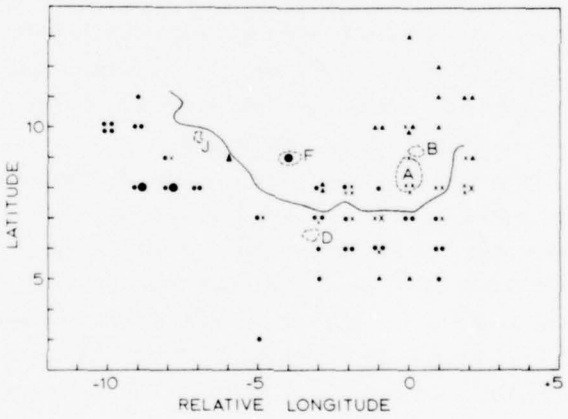


Figure 6. Locations of Flare Centroids in McMath 14943. Longitude is relative to spot A. Filled circles represent flares occurring on 9 to 15 September, crosses for 16 to 19 September, and triangles for 20 and 21 September. Small symbols indicate subflares. The configuration of sunspots and neutral line on 14 September are provided as a reference

## 4. SUNSPOT MOTIONS

Sunspot coordinates were measured from both off-band Hα and white light patrol images. In the case of the former the umbrae were measured for longitude and latitude using a Richardson film projector with movable cross hairs interfaced with the Sacramento Peak Sigma 5 computer. The coordinate reduction is based on fitting points at the solar limb; solar ephemerides are applied and the x, y coordinates of the sunspots are translated into heliocentric coordinates, corrected for geocentric parallax. The standard deviation of the distribution of coordinate measurements, made on different film frames over a small interval of time, is about 0.1 deg in both longitude and latitude for sunspots near the center of the solar disk.

The coordinates of spots A through N are given in Figure 7a, where the longitudes are relative to spot A. The latitude of the spots were also measured relative to spot A which is fixed at its mean latitude of about 8.5 degrees. Table 1 keys dates and UT to the individual points plotted in Figure 7a.

There are two principal proper motions of the sunspots in the active region: the usual stretching, in this case primarily due to the forward motion of spots A, B, C, D, F, L, M, and N (spot A moves forward in Carrington longitude by about 3.5 deg during 10 to 19 September), and a dramatic counterclockwise rotation of these same spots centered on (approximately) spot A. The large complex of forward-moving spots which participate in the rotation is not magnetically unipolar; in fact, the neutral line passes between spots D and F. However, the most rapid angular velocity appears in the unipolar pair AB, executing a 180°-rotation in seven days, including a 77°-rotation in the 44-hr period 14 to 16 September.

The stretching of the region is most rapid before 15 September. Figure 7a shows that, relative to spot A, spot G moves eastward at nearly 1 deg per day during 10 and 11 September. A similar velocity applies to the group of three small spots south of J which move along nearly parallel paths between 11 and 12 September. Finally, spot J moves more than 2 deg per day during 13 to 15 September (J is plotted in Figure 7a beginning on 14 September). Thereafter, spot J moves much more slowly and somewhat randomly, as do spots H (13 to 15 September) and K (16 to 18 September), with velocities on the order of 0.25 deg per day. It is interesting to note that the most rapid motions in the eastern part of the region cease after 15 September, coinciding with the first day of the most rapid rotation of the AB complex. This change in the locality of rapid sunspot motions also coincides in time with the cessation of flare activity in the eastern part of the region and the increase in flare activity near AB.

The rotation of the AB complex is especially significant because of the shear it generated in the vicinity of spots A and B as well as along the neutral line between spots A and D. Likewise, the stretching of the active region due to the relative

motions of the spots in the east may have generated shear there. The possible locations of sheared magnetic fields, due to these motions, are summarized in Figure 7b. Sheared fields, as evidenced by Hα fibril geometries, are further discussed in Section 9.

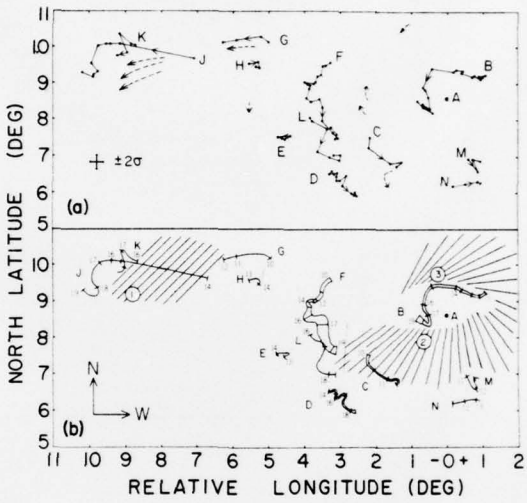


Figure 7. (a) Umbral Centroid Coordinates Derived From Off-band Hα Patrol Filtergrams. Longitudes are relative to spot A; latitudes are approximately absolute. Each dot represents a coordinate measurement for which dates and UT are given in Table 1. Dashed lines indicate motions observed on white light patrol photographs which show a few smaller spots. (b) Schematic Representation of the Active Region Showing Spot Motions and Regions Presumably Sheared (hatched areas) By Spot Motions. (The presence of shear in the western part of the active region is confirmed by fibril geometry). The widths of the bands showing motions for spots B, C, D, and F are proportional to the areas of those spots (see Figure 5); bars indicate positions of spots at approximately 1500 UT each day (dates are given by numerals). Circled numbers indicate centroids of the three flare zones

Table 1. Dates and UT for Sunspot Coordinate Points. Each asterisk indicates a datum in Figure 7a for the particular spot

| Sept | UT | A | B | C | D | E | F | G | H | J | K | L | M | N |
|---|---|---|---|---|---|---|---|---|---|---|---|---|---|---|
| 10 | 1446 | * | * | * | | | * | * | | | | | | |
| 10 | 1812 | * | * | | | | * | | | | | | | |
| 10 | 2250 | * | * | * | | | * | * | | | | | | |
| 11 | 1928 | * | * | * | | | * | * | | | | | * | * |
| 11 | 2356 | * | * | * | | | * | | | | | | | |
| 12 | 145? | * | * | * | | | * | * | | | | | * | * |
| 13 | 1404 | * | * | | * | * | * | | * | | | | * | * |
| 13 | 1735 | * | * | | * | * | * | | * | | | | * | * |
| 14 | 1435 | * | * | | * | * | * | | * | | | | | |
| 14 | 1835 | * | * | | * | | * | | * | * | | | | |
| 15 | 1409 | * | * | | * | * | * | | | * | | | | |
| 16 | 1442 | * | * | | * | | * | | | * | * | * | | |
| 16 | 1949 | * | * | | * | | * | | | * | * | * | | |
| 16 | 2243 | * | | | | | * | | | | | | | |
| 17 | 1536 | * | * | | * | | * | | | * | * | * | | |
| 17 | 1832 | * | * | | * | | * | | | * | | * | | |
| 18 | 1545 | * | * | | * | | * | | | * | * | * | | |
| 18 | 1825 | * | * | | * | | * | | | * | * | * | | |
| 18 | 2259 | * | * | | * | | * | | | * | | * | | |
| 19 | 1437 | * | * | | * | | * | | | * | | * | | |
| 19 | 1943 | * | | | | | * | | | | | | | |

## 5. EVOLUTION OF PRINCIPAL SPOTS

Flares have long been known to be associated with the rapid development of sunspots.[9] Therefore, we have measured twice daily the umbral areas of the principal spots in McMath 14943 (Figure 5). The most obvious changes are the increase in area of spot F (16 September), of spot B (17 and 18 September), and the decline in the area of spot A (16 September). These changes coincide approximately in time with the largest flares in the region (occurring on 16, 19, and 20 September). In contrast to this, one notes the significant decline in the area of spot A on 10 and 11 September which is not associated with any events larger than subflares (three flares of importance 1 occurred on 9 and 10 September but their locations were in the eastern part of the region).

The spots in the eastern part of the region show a tendency for dissipation over 9 to 20 September. This dissipation is interesting because flare activity also ceases in the east, although more abruptly than the sunspot dissipation. A comparison of the photographs in Figure 1 shows that spot G and the group of three umbrae east of G are well developed during 9 to 11 September. The latter three begin to dissipate on 12 September, while G and H persist until 14 September. Spots J and K appear on 14 and 16 September, respectively, and both start to dissipate on 18 September. The dissipation of sunspots in the eastern part of McMath 14943 is therefore not monotonic, but rather, consists of the emergence and decay of several individual spots separated in time; the overall trend, however, is toward fewer spots.

Beginning on 18 September we observe the appearance of new spots adjacent to, and north of, the AB complex. These grow steadily during 19 September and by 20 September form a penumbral annex of negative polarity north of AB. This growth occurs at a time when the areas of both A and B are decreasing. These newly-emerging spots are obviously associated with the onset of flare activity at this location during 20 and 21 September.

## 6. SMALL-SCALE CHANGES IN SPOT STRUCTURES

The emergence of new magnetic flux into an ambient field structure has been cited as a possible origin of solar flares.[19] Rust[13] described several cases where emerging flux, as determined from magnetograms or from the formation of pores, was observed in connection with flares. In this section we consider both the emergence and decay of small-scale fields in relation to flare incidence, assuming that the emergence or decay of such magnetic structures is observable in the form of the appearance or disappearance of pores or other small structures visible in white light.

19. Heyvaerts, J., Priest, E.R., and Rust, D.M. (1977) Ap. J. 216:123.

In the 10-day period 10 to 19 September a total of 77 changes (occurring on times scales of an hour or longer) were identified as possible candidates. The emergence of pores or small spots accounted for 56 of the recorded changes. During the same period of observation 24 subflares occurred, according to Solar Geophysical Data.[17] Coincidences between the locations of the candidate changes and the subflares for each day were tested for chance association by equating the fractions of the active region area (about 77 square deg) covered by the subflares to the sum of the probabilities that each of the small-scale changes would fall at random within any of the flaring areas. For the purposes of establishing a coincidence each subflare was assigned a circular area of radius 1.5 deg, equal to the square root of the upper limit area defined for subflares. Thus, a hypothetical condition was made for the triggering of flares by small-scale field changes over an area larger than the subflare itself. Flares larger than subflares were not considered here because their large and complex structures covered too much of the active region to allow a meaningful application of the coincidence test, that is, a coincidence was virtually always certain in these cases. No attempt was made to check any coincidences within a time frame shorter than an observing day (about 10 hr); thus, the test applied here assumed also the condition that the small-scale changes could occur either before or during the flare, or could even be delayed in their appearance until after the flare.

The results of the test showed that the number of daily coincidences between locations of small-scale changes and subflares, according to the hypothesis set forth, is as expected by chance association. The entire 10-day period contained 11 coincidences, whereas 15 could have been produced at random. On five of the ten days the number of coincidences was exactly as predicted by chance association. This result, in addition to the fact that six changes (all emergences) occurred on 12 September without a single flare occurring on that day, suggests that such phenomena are not physically associated. It is possible, however, that the many observed small-scale changes which were not flare associated either did not possess the magnetic properties necessary to trigger flares or were not located within the ambient fields at points where triggering could occur. Nevertheless, this observation demonstrates that great care should be taken when associating flares with other transient phenomena which are occurring profusely in active regions.

## 7. ANALYSIS OF MAGNETOGRAMS

The collection of magnetograms in Figure 4 (plus a few others not shown here) is adequate only for a coarse description of the evolution of the principal magnetic structures over the period 13 to 18 September. Specifically, we have examined the magnetograms for neutral line complexity, maximum field strengths, principal gradients, and emerging flux.

Throughout most of its transit McMath 14943 maintained an east-west orientation of the principal neutral line. However, the counterclockwise rotation of the AB complex appears to wrap the western end of the neutral line around spots AB. Comparison of the magnetograms shows little change in the neutral line over 13 and 14 September. The rapid rotation of AB, beginning on 15 September, produces changes which are quite evident on the magnetogram of 16 September. The shape of the neutral line south of spot A is also greatly influenced by the emergence of new flux at this location, producing the southward diversion and large kink visible after 16 September. Since the flare activity increased as these changes occurred. we suggest that the known association between flare incidence and neutral line complexity[20] is more likely to originate from the motions or emerging fluxes causing the neutral line complexity than from the existence of complexity itself.

Magnetic field gradients were measured at a number of points along the neutral line. All measurements at a given point were made between the isogauss contours giving the maximum gradient (average gradients, measured between spot centers, gave consistently smaller values). The largest gradient measured was a modest 0.2 G/km, occurring on 14 September (1451 UT) along the neutral line between spots E and F. We found no definable trends in the strengths of the measured gradients which could be related to flare activity. This result, however, should not be considered conclusive because of the poor time resolution and because small trends may have been masked by seeing conditions.

At least ten islands of emerging or strengthening flux were noted on the magnetograms during 13 to 18 September. These regions had sizes on the order of $10^4$ km and fluxes in the range $10^{19}$ - $10^{20}$ Mx. Table 2 summarizes their occurrence, polarity, position, and their association with the zones of flare activity discussed in Section 3. A note is also made regarding the location of the emerging flux relative to sheared magnetic fields. The presence of shear was deduced from the morphology of fibril structures (Section 9). In constructing Table 2 we note again that the magnetogram coverage is incomplete and that, given this circumstance, the evolution of the magnetic structures is difficult to track, especially in the eastern part of the region.

20. Lemmon, J.J. (1972) in Progress in Astronautics and Aeronautics, P.S. McIntosh and M. Dryer (Eds.) 30:421.

Table 2 indicates two emerging flux regions (8 and 9) which are associated with zones of flare activity. Region 8 appears first as a small inclusion of negative polarity south of the neutral line across from spot A (see magnetogram of 14 September, 2126 UT). Flux continues to grow at this point as well as south of, and adjacent to, spot A. Region 9 is associated with the formation of the penumbral annex north of spot A, and appears on the magnetograms of 18 September as a northward distention of the magnetic feature associated with spot A.

Table 2. Regions of Emerging or Strengthening Flux in McMath 14943

| Region | Date (Sept) | Polarity | Location | Associated with a zone of flare activity | Located in a sheared region |
|---|---|---|---|---|---|
| 1 | 13-14 | + | North of A | No | No |
| 2 | 14 | + | NW of F | No | No |
| 3a | 13-14 | + | NE of F | No | No |
| 3b | 13-14 | + | NE of F | No | No |
| 4 | 13-14 | - | North of F | No | No |
| 5 | 17-18 | + | NE of F | No | No |
| 6 | 16 | + | SW of D | ? | No |
| 7 | 14 | - | South of D | No | No |
| 8 | 14-16 | - | South of A | Yes | Yes |
| 9 | 18-21* | - | North of A | Yes | Yes |
| 10 | 17-18 | + | North of A | ? | No |

*We assume growth after 18 September on the basis of the new spots which continue to develop.

It is remarkable that the regions which were definitely associated with zones of concentrated flare activity were those in which the flux emergence occurred in localities which were also sheared. We consider this as possible evidence in support of the claims that new flux emerging into sheared fields is required to produce flares.[14,21] In making this statement, however, we note the following:

(1) We do not suggest that we have found necessary conditions for all flares in McMath 14943, but possibly, for two of the zones of concentrated flare activity.

(2) Only one of the emerging flux regions is associated with the development of new spots. This region was one of two associated with flare zones.

(3) The two regions associated with the flare zones (and shear) emerged very close to a major spot structure, and had the same polarities as the spot. Of the eight flux regions which were not flare associated, only two (Regions 2 and 7) were

21. Rust, D. M. (1977) American Science and Engineering Preprint No. 4218, Cambridge, MA.

located in close proximity to major sunspot structures. Thus, it could be argued that the remaining six might not have been expected to produce many flares.[12]

In view of this last point we suggest that in order to make a strong case for emerging flux-shear as a condition required for flares, we would like to observe flux emerging in similar proximity to spots, but in unsheared configurations.

## 8. ANALYSIS OF TACHOGRAMS

We were not able to find line-of-sight velocity patterns in the photosphere which were related to flare activity. However, the velocity measurements were available only for three days, and then only several times daily. The time resolution was therefore insufficient to detect the type of changes reported by Rust[10] prior to flares. Furthermore, the horizontal photospheric motions which might have been associated with the sunspot motions or shearing[22] were not observed in this case due to the region's location near disk center on the days when tachograms were available (13 to 16 September). The reader may refer to DeMastus et al[23] for a presentation of these tachograms.

## 9. FORCE-FREE MAGNETIC FIELDS

### 9.1 Energy Storage

The build-up and storage of energy in force-free magnetic fields has been described in many papers.[8] Energy in excess of a potential (minimum energy) configuration originates from currents induced by relative motions of the footpoints of magnetic flux tubes. The energy stored in the resulting twisted fields is extractable when the fields relax toward a potential configuration.

Tanaka and Nakagawa[8] described the energy build-up and release associated with the large flares of August 1972. The shearing motions (observed as sunspot motions) were also evidenced by the increase with time in the inclination angles of chromospheric fibrils (connecting the moving spots of opposite polarity) relative to a reference line drawn between the spots (representing the fibril directions corresponding to a bipolar potential configuration). Following the large flare of 7 August, smaller inclination angles were observed, indicating that a relation had occurred. Other observations[4,24] have also indicated relaxations associated with flares.

22. Harvey, K. L., and Harvey, J. W. (1976) Sol. Phys. 47:233.
23. DeMastus, H. L., Neidig, D. F., and Wiborg, P. H. (1978) UAG Report, World Data Center A, National Oceanic and Atmospheric Administration, Boulder, CO (in press).
24. Bruzek, A. (1975) Sol. Phys. 42:215.

The magnetic energy in excess of a potential configuration stored in a region of length L and width W between poles with field strengths B can be approximated by[8]

$$E = \frac{B^2 L^2 W^2}{32\pi^2 \sqrt{L^2+W^2}} (\sec \theta - 1) \text{ erg} \qquad (1)$$

where $\theta$ is the angle, measured at the neutral line, between the fibrils and a straight line connecting the poles (the latter assumed to be the projection on the solar surface of field lines in a potential configuration).[8] Equation (1) differs from Eq. (8) of Tanaka and Nakagawa[8] due to the definition of the angle used here and to the correction of an error in their original equation.[25]

### 9.2 Flares and Fibril Configurations

Since the energy build-up in force-free fields originates from photospheric motions it is reasonable to expect that sheared fields will be found near sunspots which undergo relative motions. Accordingly, we can identify two locations within McMath 14943: the eastern part of the region (motions associated with stretching) and the western part of the region surrounding spot A (sunspot rotation). It happens that the centers of all three zones of flare activity lie within these two regions of shearing motions. We first examine the region surrounding spot A for evidence of shear in the fibril configuration and its relation to the flare activity there in Zones 2 and 3.

It is evident from Figure 7 that the entire group of major spots is rotating slowly in a counterclockwise sense. However, the rotation rate of the AB complex is much greater than that of its oppositely-poled surroundings south and west of the neutral line. As a result of this differential rotation, the field lines connecting region AB with the regions near spots C and D and the plages south and west of spot A become sheared in the manner so vividly depicted by the fibrils in the photographs (Figure 3). It is even possible to see in a glance the increase in shear between 13 and 14 September. The measurements of the shear angle $\theta_1$ between A and D are referenced to a straight line drawn between spots A and D, while the shear $\theta_2$ between A and the plage south and west of A is referenced to radius vectors centered on A and averaged over a 90° sector extending southward and westward of spot A. All measurements of $\theta_1$ and $\theta_2$ were made at the neutral line and are corrected for foreshortening.

The onset of a small flare (importance -N), spanning the neutral line south and west of spot A, is visible on 14 September, 1541 UT. A simple comparison with the region at 2239 UT shows an apparent relaxation of shear following this flare.

25. Nakagawa, Y. (1978) Private communication.

Corresponding values for $\theta_2$ are given in Table 3. It is further noted that the relaxation is confined to the region of the flare (according to the definition of $\theta_2$), while at the same time the fibrils associated with $\theta_1$ actually show a slight increase.

Table 3. Physical Parameters for the Flares With Observed Relaxation

| Date | UT | $\theta_1$[a] | $\theta_2$[a] | L(cm)[b] | W(cm) | Scaling factor | B (gauss) (-) (+) | Energy[c] (ergs) |
|---|---|---|---|---|---|---|---|---|
| Sep 13 | 1400 | 45 | 48 | | | | | |
| 14 | 1400 | 63 | 57 | $3.1 \times 10^9$ | $1.6 \times 10^9$ | 1/4 | 2500/320 | $3.7 \times 10^{30}$ |
| 14 | 2300 | 68 | 45 | $3.1 \times 10^9$ | $1.6 \times 10^9$ | 1/4 | 2500/320 | $2.8 \times 10^{30}$ |
| 15 | 1945 | 78 | | | | | | |
| 16 | 2025 | 77 | | $4.6 \times 10^9$ | $1.6 \times 10^9$ | 1/2 | 2500/1600 | $1.25 \times 10^{32}$ |
| 17 | 1335 | 64 | | $4.6 \times 10^9$ | $1.6 \times 10^9$ | 1/2 | 2500/1600 | $4.6 \times 10^{31}$ |

[a] Angles were measured from high resolution Hα filtergrams on 13 and 14 September, and from patrol images on 15 to 17 September.

[b] For the subflare of 14 September L is the center-to-center distance between spot A and the plage to the southwest of A; for the 16 September flare we use the distance between spots A and D.

[c] The product of B(-) and B(+) was substituted for $B^2$ in Eq. (1).

The principal interest in $\theta_1$ is the 2N flare which occurred along the neutral line between spots A and D on 16 September, 2141 UT. Since high resolution filtergrams were not taken after 14 September, we present instead a sequence of daily Hα patrol images covering the period 14 to 17 September (Figure 2). The resolution of these is sufficient to show only the neutral line filament which we can assume to be aligned approximately with the field lines (note the striations in the vicinity of this filament in Figure 3). The increase in $\theta_1$, evident in the neutral line filament, is clearly seen during 14 to 16 September (see also Table 3). However, the increase may not be monotonic during this period, as a number of subflares occurred at this location. Two subflares occurred between the times of the photographs on 14 and 15 September, and five occurred between the photographs of 15 and 16 September. Relaxations, possibly associated with these subflares, would oppose the expected increase in $\theta_1$ due to the rotation of AB. This may explain the apparent lack of change in $\theta_1$ between 15 and 16 September. Unfortunately, no photographs

were available immediately after the 2N flare, which occurred late in the afternoon of 16 September. The next available photograph (1335 UT, 17 September) shows a relaxation of about 13 deg in $\theta_1$. Furthermore, the filament is now split and resembles the less-sheared configuration of 13 September. Since the time of this measurement is a half-day after the flare we should be aware that $\theta_1$ could have increased from its post-flare value due to the rotation of AB. However, Figure 7 indicates that the rotation has slowed considerably by this time and therefore $\theta_1$ is probably similar to its post-flare value.

The energy release associated with the relaxations observed in the flares of 14 and 16 September are approximated by Eq. (1). The values for the lengths, widths, field strengths, angles, and energies are summarized in Table 3. The choice of the width W is based on the diameter of spot A, which is the negative pole for the flux in the case considered. Geometric scaling factors are applied since the magnetic flux terminating in spot A is obviously partitioned among several positive poles. Accordingly, we have assumed half of the flux to be connected to the strong positive pole in the region near spot D. From inspection of the high resolution photographs we assume the remaining half to be connected in the network to the north, west, and south of spot A, with about a fourth of the flux connecting the plage southwest of A (which involved the subflare).

The difference in the force-free field energies before and after the flares are $10^{30}$ and $8 \times 10^{31}$ erg for the subflare and the 2N flare, respectively. These energies are compatible with the energies released in flares of these sizes.

The optical emission in the subflare was confined within an area roughly equivalent to an area LW, wherein the relaxation was observed. In the case of the 2N flare, however, the emission extended far beyond the region similarly defined. This raises the question whether the released energy propagated over large distances from the region where the relaxation occurred or whether the relaxation, in fact, occurred over a much larger area but was simply not able to be observed. Since the large flare was observed only with the low resolution patrol telescope we are unable to distinguish between these two possibilities.

In comparing the sizes of the two flares with the preflare extractable energies we find, not unexpectedly, that the larger flare occurred at the location of greater extractable energy (Table 3). This relationship extends also to the case of the 3B flare[8] where the preflare energy was $\geq 2.2 \times 10^{32}$ erg, obtained after correction of errors in the calculated energies.[25] We therefore suggest that the near real-time monitoring of the stored energy might provide a useful forecasting tool, namely, a knowledge of the upper limit energy of potential flares at each location of shear.

The onset of flare activity north of spot A (Zone 3) is not simultaneous with the activity in Zone 2. Although the fibrils in Zone 3 are sheared the flares nevertheless do not occur during the period of rapid rotation of AB, but appear only later when the

new spots form. This appears to be a clear case of major flux emergence into a region which had been previously sheared.

In the eastern part of the region we observe rapid sunspot motions during the period in which flares were occurring in Zone 1. However, in this case the motions may only have stretched the field lines instead of producing shear. In witness of this, one notes the strong filamentation, connecting spot J with the opposite polarity near spot F (Figure 3, 14 September), which exhibits virtually no shear ($\theta \simeq 0°$). On the other hand, the magnetograms of 14 September show a negative pole positioned north of spot J. This pole did not produce any significant spots and therefore it is not easy to determine whether the pole moved parallel with spot J (producing no shear) or whether there was a shear-producing differential motion. A careful examination of the high resolution filtergrams reveals the possible presence of sheared fibrils in a small region just northwest of spot J. Thus, while the eastern part of the region contained some of the ingredients required to produce shear, we are not able to present a strong case for its existence.

## 10. PRINCIPAL CONCLUSIONS

We identify the evolution of flare activity in three zones within McMath 14943, and find some evidence that a combination of both sheared fields and emerging flux is associated with flare incidence. The zone of activity south of the large preceding spot was subjected simultaneously to shear and emerging flux. The zone north of the preceding spot was subjected first to rotational shear, but flares did not develop there until several days later when new magnetic flux emerged. The zone of activity in the eastern part of the region did not present a clear-cut case and thus produced no conclusions.

The regions of emerging flux which were flare associated were relatively large in size ($\sim 10^4$ km) with fluxes on the order of $10^{19}$-$10^{20}$ Mx. Small-scale flux changes, assumed to be evident as emerging pores or other small-scale spot changes, were found to be randomly associated with flares. Thus, we suggest that the emerging flux regions associated with flares may be exclusively limited to major entities, and further, that the monitoring of either pore emergence alone or small-scale spot structures alone may not be an effective means for identifying flare-producing zones within active regions.

Evidence is found for the role of force-free magnetic fields in the storage of flare energy. We have identified the possible energy build-up in sheared fields prior to the occurrence of both a subflare and a large (2N) flare. We have further identified the relaxation in shear following these flares. Estimates for the differences in stored energy, before and after these flares, were in good agreement with the energy release in each.

We have no a priori reason to ignore the fact that the flares in the western part of McMath 14943 were occurring at the same time the major spots A, B, and F were changing in size. On the other hand, the association between local flare activity and the presence of shear and emerging flux seems somewhat more direct and persuasive. It is curious, though, that (with the exception of the decline in the area of spot A on 10 and 11 September) the changes in spot areas tend to occur during the periods of spot motions. This effect, which might be purely coincidental, is noticeable in comparing Figures 5 and 7. In addition, we note the dissipation of spots (and flares) in the eastern part of the region following the reduction there in the spot motions. This raises the question whether these two phenomena might be related in some way.

The association found between the zones of flare activity, sunspot motions, shear, and emerging flux suggests that near real-time monitoring of these same quantities could lead to improvements in the forecasting of flares. The capability for such 24-hr monitoring of these quantities will exist in 1980 when the USAF Air Weather Service completes its five-site Solar Observing Optical Network (SOON).

## References


1. McIntosh, P.S. (1969) Report UAG-5, World Data Center A, National Oceanic and Atmospheric Administration, Boulder, CO, p 14.
2. McIntosh, P.S. (1970) Report UAG-8, World Data Center A, National Oceanic and Atmospheric Administration, Boulder, CO, p 22.
3. Zirin, H., and Lazareff, B. (1975) Sol. Phys. 41:425.
4. Tanaka, K. (1976) Sol. Phys. 47:247.
5. Sakurai, K. (1976) Sol. Phys. 47:261.
6. Stenflo, J.O. (1969) Sol. Phys. 8:115.
7. Sturrock, P.A. (1972) in Progress in Astronautics and Aeronautics, P.S. McIntosh and M. Dryer (Eds.), 30:163.
8. Tanaka, K., and Nakagawa, Y. (1973) Sol. Phys. 33:187.
9. Giovanelli, R.G. (1939) Ap. J. 89:555.
10. Rust, D.M. (1973) Sol. Phys. 33:205.
11. Martres, M.J., Michard, R., Soru-Iscovici, I., and Tsap, T.T. (1968) Sol. Phys. 5:187.
12. Vorpahl, J.A. (1973) Sol. Phys. 28:115.
13. Rust, D.M. (1974) AFCRL-TR-74-0201.
14. Rust, D.M., Nakagawa, Y., and Neupert, W.M. (1975) Sol. Phys. 41:397.
15. Dunn, R.B. (1971) Solar Magnetic Fields, R. Howard (Ed.) IAU Symp. 43:65.
16. Beckers, J.M., Dickson, L., and Joyce, R.S. (1975) AFCRL-TR-75-0090.
17. Solar Geophysical Data, World Data Center A, National Oceanic and Atmospheric Administration, Boulder, CO.
18. McIntosh, P.S. (1977) Bull. Am. Astron. Soc. 9:330.
19. Heyvaerts, J., Priest, E.R., and Rust, D.M. (1977) Ap. J. 216:123.
20. Lemmon, J.J. (1972) in Progress in Astronautics and Aeronautics, P.S. McIntosh and M. Dryer (Eds.) 30:421.

21. Rust, D. M. (1977) American Science and Engineering Preprint No. 4218, Cambridge, MA.

22. Harvey, K. L., and Harvey, J. W. (1976) Sol. Phys. 47:233.

23. DeMastus, H. L., Neidig, D. F., and Wiborg, P. H. (1978) UAG Report, World Data Center A, National Oceanic and Atmospheric Administration, Boulder, CO (in press).

24. Bruzek, A. (1975) Sol. Phys. 42:215.

25. Nakagawa, Y. (1978) Private communication.